Materials and Design 199 (2021) 109427

Contents lists available at ScienceDirect

Materials and Design

journal homepage: www.elsevier.com/locate/matdes

Reactive in-situ formation and self-assembly of MoS_2 nanoflakes in carbon tribofilms for low friction

Bernhard Kohlhauser [a,b,1], Carmen I. Vladu [c], Carsten Gachot [d], Paul H. Mayrhofer [b], Manel Rodríguez Ripoll [a,*,1]

[a] AC2T research GmbH, 2700 Wiener Neustadt, Austria
[b] Institute of Materials Science and Technology, TU Wien, A-1060 Vienna, Austria
[c] CEST Centre for Electrochemistry and Surface Technology GmbH, 2700 Wiener Neustadt, Austria
[d] Institute of Engineering Design and Product Development, TU Wien, A-1060 Vienna, Austria

HIGHLIGHTS

- Raman spectroscopy shows the formation of MoS_2 by the tribochemical reaction between Mo disks and S-additives.
- In situ reactive formation of MoS_2 nanoflakes reduces friction down to 0.06.
- Low friction caused by a only few self-assembled and (002)-oriented monolayers of MoS_2.
- Raman and TEM analyses reveal MoS_2 accompanied by catalytically formed carbon tribofilms at temperatures above 100 °C.
- Stable friction coefficient of 0.08 maintained at temperatures of 130 °C without oxidation of the MoS_2 nanoflakes.

GRAPHICAL ABSTRACT

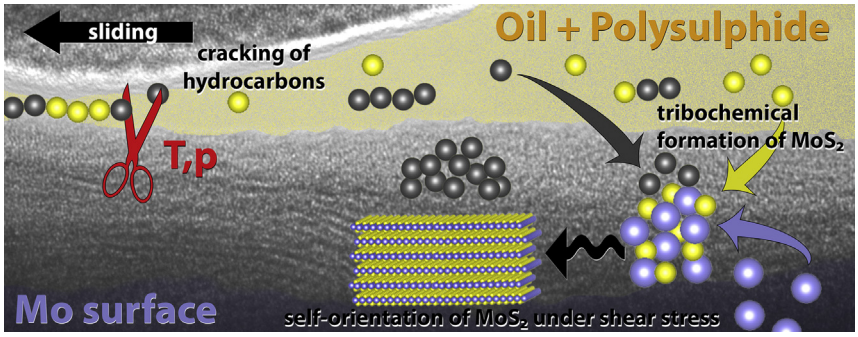

ARTICLE INFO

Article history:
Received 11 September 2020
Received in revised form 17 December 2020
Accepted 18 December 2020
Available online 22 December 2020

Keywords:
MoS_2
In-situ formation
Tribofilm
Catalytic surface
Solid lubrication

ABSTRACT

Modern lubricants require additives for improving their frictional and wear performance. The most effective and widely used additives rely on organo-metallic compounds, which lead to ash formation and pose serious environmental concerns. Despite intensive research, a cost-effective alternative cannot be foreseen in the immediate future.

On the quest for an alternative concept, the reactive formation and self-assembly of few-layer MoS_2 nanoflakes in a carbon-based tribofilm is studied during reciprocating sliding contact of molybdenum substrates lubricated with oils containing sulfurized olefin extreme-pressure (EP) additive. Based on a combination of Raman spectroscopy and transmission electron microscopy it can be concluded that nanoflakes of well-adherent 002-oriented MoS_2 layers form in the presence of S-containing EP additive. This leads to a reduction in friction from 0.3 to 0.08. The reaction rate to form MoS_2 nanoflakes increases with temperature and EP concentration. At temperatures over 100 °C, the MoS_2 nanoflakes are accompanied by carbon-based tribofilms. These carbon-based tribofilms are catalytically formed by dissociating hydrocarbon molecules of the lubricant.

These results suggest that applying Mo alloyed materials with sulfur containing lubricants provides an alternative to conventional organo-metallic compounds. The presented lubrication concept can be utilized for further developments of materials (like protective hard coatings) and machine designs.

* Corresponding author at: AC2T research GmbH, 2700 Wiener Neustadt, Austria.
E-mail address: ripoll@ac2t.at (M. Rodríguez Ripoll).
[1] B·K and M.R.R. contributed equally to this work.

https://doi.org/10.1016/j.matdes.2020.109427

1. Introduction

Modern machine designs require further synergies between materials and lubricants. Tighter environmental regulations (e.g., in the automotive sector) promote the application of ultra-low viscosity oils such as 0W10, leading to thinner lubricating oil films. While this reduces any losses within the lubricant films, the risks for direct metal-to-metal contacts increase. Especially in these boundary lubricated regimes, the formation of protective tribofilms is essential to increase the component lifetime. Current lubricants rely on functional friction modifiers and anti-wear additives to meet the increasing demands for lower friction and wear.

Commercially prevailing oil additives such as zinc dialkyl dithiophosphate (ZDDP) [1] equip lubricants with excellent wear protection (especially under boundary lubricating conditions) [2,3] as well as other beneficial properties such as corrosion protection. However, ZDDP as well as the often used molybdenum dithiocarbamate (MoDTC) friction modifier (which forms lubricious MoS_2 platelets) rely on organometallic compounds [4–6]. These form ashes in combustion engines and can harm after-treatment and fine-particle traps, besides having serious environmental concerns. Unfortunately, alternatives at a similar cost are still out of reach [7]. Additionally, many of the well-established additives can only unfold their potential when in contact with ferrous surfaces [8]. This limits their potential in modern machine design with its massive move towards lightweight materials and components having protective coatings.

Therefore, recent research concentrates on the development of multifunctional triboactive surfaces to enable low friction while still ensuring the required wear protection. Such triboactive surfaces are themselves essential for the tribofilm formation and mimic some of the classical roles of lubricant additives. In their seminal work [9], Erdemir et al. showed that triboactive thin films catalytically modify the surrounding medium to produce oil-derived carbon-based tribofilms. More recently, oil-derived carbon based tribofilms were also achieved from ambient hydrocarbons using Pt–Au coated steel sliding against alumina in dry contact conditions [10]. Similar lubricious and wear protective carbon-based tribofilms form via high molecular weight hydrocarbons when cyclopropanecarboxylic acid is used as lubricant additive [11,12]. In addition to such oil-derived carbon-based tribofilms, also the tribochemical formation of other 2D materials like transition metal dichalcogenides (TMD) such as MoS_2, WS_2, $MoSe_2$, or WSe_2 is studied. Their layered structure of alternating transition metal and chalcogen atoms allows for easy shear resulting in low friction [13–16]. Such TMDs can directly be deposited as protective coatings [17–20], or simply be added to lubricants in form of nanoparticles [21–24]. Major concerns of the former approach is that humidity degrades the frictional performance of those coatings, while the latter approach suffers from antagonistic interactions between the TMD nanoparticles and the dispersants required to produce stable emulsions [25–27].

Alternatively, TMD can elegantly be formed in-situ by tribochemical reactions [28–30], a concept that has its roots in 1996, where pioneering studies showed the tribochemical formation of MoS_2 when applying Mo-containing surfaces in H_2S atmospheres [28,31,32]. With the commercial success of W-doped DLC coatings, similar concepts extracted the formation of protective W and S containing tribofilms with S containing additives [29,33–35]. Corresponding low-friction tribofilms can also be achieved with WC-containing surfaces [30]. In contrast to TMD coatings whose friction behavior is highly dependent on humidity, a main advantage of the reactive formation of TMD in lubricated contacts is that is not sensitive to humidity, a feature shared with lubricants containing TMD nanoparticles as additives. Based on these studies, we demonstrated the formation of WS_2 on wear resistant WN coatings, and highlighted the importance of oxygen availability and the formation conditions for this tribochemical reaction [36]. Those investigations also showed that the formation conditions required for disulfides are more favorable in Mo-containing coatings when compared to W-containing surfaces. With Mo being a widely used alloying element it became clear that a precise understanding of the reaction kinetics for the formation of MoS_2 is essential for exploiting this lubrication concept in future engineering applications.

Mo disks are used in order to establish a model-system for a lubricated contact (with a sulfur-containing additive) sliding against a ball counterbody. Commercially available extreme pressure (EP) additives are used as S delivery system. This EP additive is originally designed to react with ferrous surfaces under extreme pressure conditions and prevent metal-to-metal contact. However, in the present work we are pursuing the reactive formation of low-friction MoS_2 nanoflakes, so that the S-containing additive essentially has the role of a friction modifier. The use of pure Mo disks along with a base oil containing a single additive serves to focus the research on a particular tribochemical reaction (formation of MoS_2) and simplifies the post-test surface chemical analyses. The parametric analysis performed should be a solid basis for determining the conditions that favored the tribochemical formation of MoS_2 in order to find suitable ranges of application in technologically relevant components made of steel for example.

The proposed research has an enormous potential for the design of future low friction components with a higher efficiency and a lower energy consumption. These components will rely on the presence of triboactive elements, such as Mo and W, which are needed for the formation of MoS_2 and WS_2 low friction tribofilms. Such triboactive surfaces can readily be design using coatings deposited by physical vapor deposition such as WN [36], or MoN. Also commercially available thermal spray coatings containing Mo could benefit from the presented approach. Even steel can also be turned into a triboactive surface by embedding WC particles, resulting in the formation of WS_2 and profiting from the mechanisms here described [30,37,38]. The extrapolation of our lubrication concept to steels, other alloys containing Mo and/or W as alloying elements, or even to Mo and W alloys [39–42] seems also attainable, encouraged by the pioneering studies performed in the 1990s that resulted in the formation of MoS_2 and WS_2 under dry contact conditions in H_2S atmosphere [32]. The proposed lubrication concept can also be applied for the development of novel lubricants with environmentally more friendly S-containing molecules. Our previous studies have shown that the in-situ formation of MoS_2 (or WS_2) was successfully achieved with allyl-disulfide, a compound typically found in garlic, or with the amino acid methionine [37,38]. In all mentioned cases, the proposed friction reducing mechanism relies on the simultaneous presence of Mo or W in the material and S in the lubricant since the lubricant additive alone is not sufficient for reducing friction [30,37,38]. However, by doing so, Mo and W are bound to the substrate and eliminate the need for using noxious organomolybdenum friction modifier compounds in the lubricant.

2. Materials and methods

2.1. Materials and lubricants

Lubricated reciprocating sliding experiments of a mirror-polished Mo disk (details in the next paragraph) against steel balls (10 mm diameter, AISI 52100) and Si_3N_4 balls (10.3 mm diameter) were conducted with an SRV tribometer (Optimol, Germany). The reciprocating frequency was 10 Hz, the oscillation amplitude was 1 mm, and the normal force was 10 N (resulting in an initial mean contact pressure of 0.76 GPa for the steel ball and 0.88 GPa for the ceramic ball counterbody). In general the experiments were conducted at a temperature representative for engine oils (100 °C), while a temperature variation (23, 40, 100, and 130 °C) was also used to study the role of the system temperature on the tribofilm composition and frictional performance. For each parameter set, three independent measurements were conducted and averaged.

A forged molybdenum rod (hardness of 230 HV 10, Young's modulus of 320 GPa, and 99.97% purity, from Plansee SE, Austria) with 25 mm diameter was cut into discs of 7 mm thickness. These were mirror-polished to a surface roughness of $R_a = 11 \pm 3$ nm and used as base material for our reciprocating sliding tests. Bearing steel balls (AISI 52100) with a diameter of 10 mm and a hardness of 63 HRC as well as Si_3N_4 balls (grade 5) with a diameter of 10.3 mm served as counterbodies.

The lubricant used was a poly-alpha-olefin oil (PAO 8) with a viscosity of 45.5 and 7.9 mm^2s^{-1} at 40 and 100 °C, respectively. Oils with four different extreme pressure (EP) additive contents of 0, 1.5, 3, and 5 wt% were used. The commercially available EP additive (LZ 5340 MW, Lubrizol, USA) is based on sulfurized olefin polysulfide and contained 40 at.% S.

2.2. Surface characterization

After the reciprocating sliding tests, the samples were gently rinsed with n-heptane (to remove residual lubricant without damaging any formed tribofilm) for detailed Raman investigations with a LabRam ARAMIS (Horiba, Japan) Micro-Raman spectrometer. The samples were excited with a 532 nm wavelength laser (laser power of 2 mW) and measured from 100 to 3200 cm^{-1} with a 1200 $g \cdot mm^{-1}$ grid.

The worn surfaces were additionally investigated with a Leica DCM 3D confocal microscope (Leica Microsystems GmbH, Germany) for measuring the wear volumes. Based on surface topography measurements, the removed wear volumes were determined as the difference between the untested flat surface (reference) and the worn surface. The reported values for all test conditions are the average of three measurements.

High-resolution transmission electron microscopy (HR TEM) investigations were conducted with a TECNAI F20 field emission TEM (FEI, USA) in imaging, diffracting and scanning mode using an acceleration voltage of 200 kV. Prior to the analyses, the samples were protected with a Pt layer and subsequently a lamella was milled perpendicular to the sliding direction with a Quanta 200 3D DualBeam focused ion beam (FEI, USA). Since S–K lines overlap with Mo-L lines in EDX spectra, EELS was conducted for chemical investigations. The loss spectra were obtained with a GIF Tridiem (Gatan, USA) and quantified on the core losses at energies of 165 eV and 227 eV for the S-L2,3 edge and the Mo-M4,5 edge, respectively.

X-ray photoelectron spectroscopy (XPS) analyses were performed on Mo disks and steel balls using a Theta Probe equipped with a monochromatic Al Kα X-ray source ($h\nu = 1486.6$ eV) and Ar + ion gun (Thermo Fisher Scientific, USA). The base pressure inside the XPS chamber was kept constant at values in the range of 10^{-7} Pa during the measurements. The investigated samples were measured after the experiments in as-tested condition after gentle rinsing with n-heptane and after sputtering in the XPS chamber using soft Ar + for 20 s, with 3 kV and 1 μA sputter current in order to remove surface contaminants (ca. 1 nm depth). A pass energy of 50 eV was used for the high resolution spectra and the resulting binding energies were referenced to adventitious carbon at a binding energy of 284.6 eV.

3. Results and discussion

3.1. In-situ formation of MoS_2 as function of additive concentration

Pin on disk tests with steel balls on Mo surfaces at 100 °C, Fig. 1a, show a high coefficient of friction (COF) of ~0.3 when using oil without EP additive. The EP additive containing oils immediately lead to steady-state COF values of 0.08. Based on Raman spectroscopy, Fig. 1b, the reduced COF can be correlated with the presence of MoS_2, for which a Raman shift at 383 cm^{-1} (in-plane E^1_{2g} mode) and 408 cm^{-1} (in-plane A_{1g} mode) is expected [43]. The missing Raman peaks at lower and higher wavenumbers suggest that the formed MoS_2 is plate-like with only a few MoS_2 layers in thickness. MoS_2 nanoparticles would yield

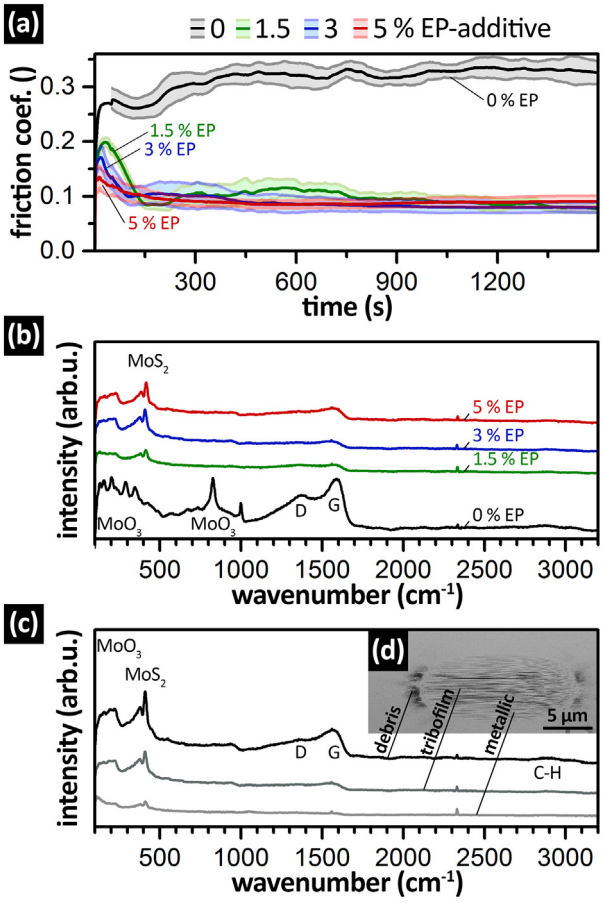

Fig. 1. Influence of the EP additive concentration during lubricated reciprocating sliding of a steel ball against a mirror-polished Mo disk at 100 °C. (a) Evolution of the coefficient of friction (COF) and (b) Raman spectra of the tribofilms after the experiment. (c) Raman spectra of regions at the rim of the contact area (labelled metallic), in the center of the contact area (labelled tribofilm), and accumulated wear debris, after the experiment with a 3% EP additive containing oil. A corresponding top view light optical microscope image of the entire wear track showing these areas is given in (d).

peaks with a wider full width at half maximum (FWHM) and slightly downshifted signals [44,45]. At the same time, partially overlapping signals from FeS_2 (at 342, 378 and 429 cm^{-1}) [46] cannot be responsible either, since the missing peak at 342 cm^{-1} suggests that its content is only small (if present at all). Highly oriented MoS_2 thin films exhibit a broad Raman peak at ~445 cm^{-1} [47], which is not the case here. Thus, the distinct Raman pattern suggests defected crystalline order for the formed MoS_2, which can also be seen in the peak structures at low wavenumbers around 227 cm^{-1}, where the broken crystal symmetry can activate (due to the Raman selection rules) Raman-inactive modes [44,45]. A similar behavior was also found for graphitic carbon materials [48].

In addition to the lower COF, the MoS_2 containing tribofilm also leads to a smoother running-in and steady-state value with increasing concentration of EP additive, which is highlighted by their lower standard deviation, Fig. 1a. The increasing intensity of the MoS_2 Raman signals with increasing EP additive content indicates increasing fraction within the tribofilm formed. This is also connected with a decreasing running-in period (until the steady-state friction is reached), because reaction rates are concentration dependent. The experiments without the EP additive show massively more molybdenum oxide (MoO_3) and no MoS_2. Consequently, and supported by the conclusions presented in [36] that the reaction pathway to form MoS_2 relies on intermediate oxide formation, MoO_3 is steadily transformed towards MoS_2 by the EP additive.

Interestingly, the contact area during our experiments without EP additive turned dark due to the formation of a carbon-based tribofilm, as proofed by Raman spectroscopy (Fig. 1b) showing the characteristic D and G band structures at 1379 and 1587 cm^{-1}. The center position of the G band (X_G) and the intensity ratio between D and G peaks (I_D/I_G) (often used as a defect index) suggest an amorphization of stage 1 (graphite to nanocrystalline graphite) or stage 2 (nanocrystalline graphite to hydrogenated amorphous carbons) according to Ferrari and Robertson [49]. The absence of a G' band at around 2700 cm^{-1} indicates that the carbon-based tribofilm could corresponds more to stage 1 and therefore be based on graphite to nanocrystalline graphite (sp^2-bonded carbon); only a small fraction of C–H bonds can be noticed with the Raman shift at 2900 cm^{-1}. Raman spectroscopy of the black wear debris (accumulated at the turning points of the reciprocating sliding test) match results of tribofilms formed on diamond-like-carbon or MoN_x–Cu coatings [9]. The precise nature of these carbon-derived tribofilms is controversial. While pioneering works attributed the Raman D and G signatures to the presence of graphitic or DLC tribofilms [9,10], a recent work [12] has shown strong experimental evidence that this C products are high-molecular weight hydrocarbons acting as solid lubricant. These products present an identical Raman spectra as DLC, with peaks around 1350 and 1580 cm^{-1} but contrastingly, they decompose at temperatures of around 350 °C.

In the tribofilms formed during lubricious contact with EP-additive-containing oils also carbon-based structures can be identified, but with a considerably smaller quantity (smaller characteristic features in the Raman spectra). The MoS_2-to-carbon intensity ratios suggest that the formation of MoS_2 and carbon structures are competing effects, with MoS_2 being dominant for EP containing oils. Interestingly, for the experiments with EP containing oils, the Raman spectra of the tribofilms show increasing G band intensity with increasing EP additive concentration. Consequently, decomposition of higher additive concentrations – for the reaction between S and Mo – also leads to higher amounts of carbon-based fragments. These presumably smaller fragments can be transformed to carbon structures causing higher G band peaks. However, the reactive formation of MoS_2 decreases the catalytic activity of the Mo surface for breaking hydrocarbons and therefore the characteristic D and G band structure massively decreases in intensity when changing from the oil without EP additive to those with (please remember, S from the EP is required to form MoS_2).

The wear scars formed by the reciprocating sliding test consist of groves and micro ploughed regions, due to the relatively high ductility and low hardness of Mo when compared to hard coatings. Therefore, any carbon-containing tribofilm that is formed on the Mo surface (as mentioned above, derived from hydrocarbons) is buried in surface ploughs or worn away and settles in the surrounding debris. Hard coatings could provide sufficient support to unfold the lubricious potential of the carbon-based tribofilm formation, as observed in [9]. Raman spectra, Fig. 1c, of three characteristic areas of the wear track (at the rim, in the center, and from accumulated debris, as marked in the overview light optical microscopy image, Fig. 1d), show the different intensities for MoS_2 and carbon structures. The wear debris give the highest intensities for Raman features indicative for MoS_2 and carbon structures. In the center of the wear track, especially the signal from carbon structures is weak. At the rim of the wear track, no intensities from carbon structures can be detected, whereas there are still features indicative for MoS_2. This indicates a better adhesion of MoS_2 when compared to graphitic structures, because the latter are constantly removed and deposited as wear debris, which therefore gives a high corresponding Raman feature. There is strong experimental evidence showing that van der Waals interactions cause strong adhesion of MoS_2 platelets to metallic substrates [50,51]. This explains why the COF is markedly lower when using EP-additive-containing oils, which allow for the formation of MoS_2. Without EP additives, only the carbon structures can act as friction modifiers, but these structures have a weaker adhesion than MoS_2.

3.2. Role of lubricant temperature on the formation of MoS_2

The lubricant temperature has a clear influence on the reactive formation of MoS_2 and on the resulting tribological properties of the tribofilm, see Fig. 2a. Experiments at 130 °C exhibit an extraordinary stable and reproducible low COF of ~0.08. At higher temperatures many chemical reactions proceed with a significantly increased rate, as thereby the necessary activation energy is easier reached and kinetic restrictions can be overcome. As a consequence, the growth rate of tribofilms results also in an Arrhenius dependency, as experimentally observed [11,52]. The interfacial temperature in a tribological contact also varies with applied load, which in our case was kept constant, due to the contribution of flash temperatures. Although our investigations show crystalline MoS_2 structures (being highly defected as suggested by Raman spectroscopy), previous studies indicate their crystallization from amorphous state due to high shear stresses and temperature active during tribological contacts [53,54]. The results also show that even though the COF is considerably higher at lower temperatures (23 and 40 °C), the consistent intensities of the MoS_2 Raman peaks (Fig. 2b) suggest the presence of MoS_2 in all tribofilms. The COF differences cannot be explained by oil viscosity differences, thus, we propose that the higher diffusivity (at higher temperatures) enhances self-assembly of MoS_2 [53]. The difference in oil viscosity may also be the reason for the slightly higher COF measured at 40 °C compared to 23 °C, even though both values are fairly close.

Based on these observations, we can conclude that the elevated temperature is a key factor for the reactive formation and self-assembly of MoS_2 layers, leading to a very stable and reproducible low friction. This behavior is intrinsically different to the one observed in nanolubricants containing transition metal dichalcogenide (TMD) nanoparticles. There, an increase in temperature degrades the tribological performance of the TMD tribofilms, due to oxidation of MeS_2 to MeO_3 (with Me = Mo, W) [55]. In both cases, the tribofilms contain a few self-assembled TMD layers. The main difference is that TMD nanoparticles produce the tribofilm by exfoliation of platelets from them, while in our case the layers of MoS_2 are produced reactively. The presence of EP additive during the test allows for a continuous in-situ re-sulfurization of molybdenum oxide, as observed in [56,57], therefore higher temperatures are beneficial.

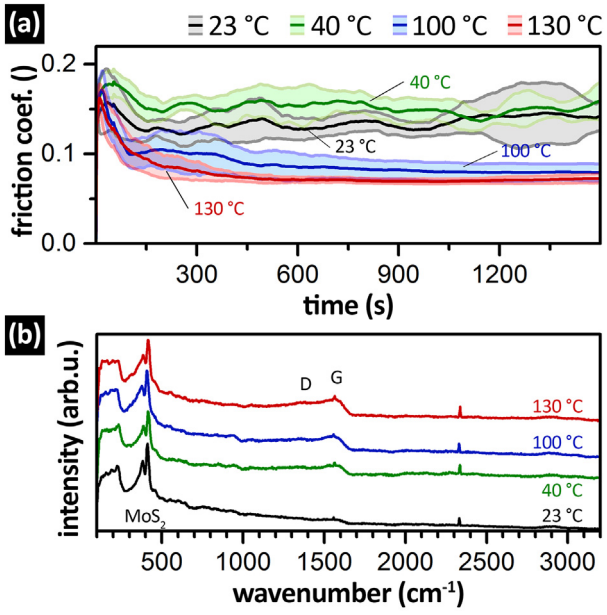

Fig. 2. Influence of the contact temperature on friction and tribofilm formation during contact with a 3% EP additive containing oil against a steel ball. (a) Lower coefficient of friction and (b) stronger carbon-based Raman signals with higher temperatures.

The results obtained here further suggest that the higher temperature (hence, allowing to easier reach the necessary activation energy) also promotes formation of carbon-derived structures. Besides temperature, the growth rate of this carbon-derived tribofilms is determined by the shear stresses [11]. If we consider a reduced shear caused by the presence of the now active MoS_2 lubrication (which could also locally decrease flash temperatures) the higher overall temperature also causes a reduced oil viscosity. Thereby, single asperity contacts increase resulting in severe shear conditions locally, by which tribochemical reactions are supported again. This comparison of temperature effects (externally applied and internally generated) highlights the huge complexity of frictional effects and their dependence on simple changes (like temperature); an enormously dynamic process.

3.3. Role of the counterbody on friction

To impart severe contact conditions, the tribological experiments were repeated with an oil containing 3% EP additive at room temperature and at 100 °C, but now using a ceramic Si_3N_4 ball. The hard and inert counterbody not only eliminates any potential tribochemical role of the iron surface, but also simultaneously allows for a higher contact pressure (because it experiences nearly no flattening due to its negligible wear). Initially, the coefficient of friction (at 100 °C) is as low as 0.06 but steadily increases to around 0.1, Fig. 3a. At room temperature, the COF starts at 0.08 but rapidly increases to 0.1 after the first initial sliding cycle (which takes about 100 s). However, in the long run (after 300 s) the COF is lower than at 100 °C.

The room temperature experiments show that although the Raman peaks characteristics for MoS_2 are significantly lower with a Si_3N_4 ball, the COF is well below the value obtained with a steel ball (compare Fig. 3a and b). It should be noticed that correlation between the intensity of the Raman peaks and the tribofilm performance is not straightforward. As shown in Fig. 1c, the regions with a higher Raman signal are those with accumulated debris at the turning point of the wear scar. This suggests that a higher Raman intensity may arise due to a higher formation together with a higher removal rate of MoS_2. In

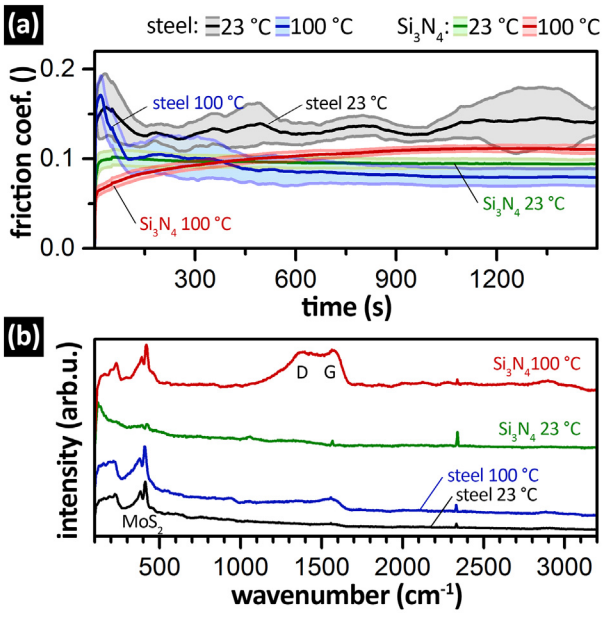

Fig. 3. Influence of the counterbody on friction and tribofilm formation during contact with a 3% EP additive containing oil at room temperature (23 °C) and 100 °C. (a) The temperature has a stronger effect on the COF against steel than Si_3N_4 balls. (b) At 100 °C the carbon-based Raman signals are stronger when using Si_3N_4 instead of steel balls, whereas at room temperature no carbon-based Raman signals can be detected when using Si_3N_4 or steel balls. Contrary, the MoS_2 Raman signal is significantly stronger (even at 23 °C) when using steel instead of Si_3N_4 balls.

case of using a Si_3N_4 ball, its higher deformation resistance leads to a smaller contact area and more severe conditions in the contact, favoring the formation of a stable MoS_2 tribofilm. At 100 °C, the Raman spectra show comparable MoS_2 signals but significantly different carbon-based signals for Si_3N_4 and steel balls. With a Si_3N_4 counterbody, the D and G bands have a ratio of almost 1:1 and their intensity is larger when compared to the experiments performed with a steel ball. Consequently, the formation of MoS_2 and carbon products is supported by higher temperatures. Although MoS_2/graphene heterostructures have been investigated for their superlubricity [58], the increased intensity of the Raman peak at 227 cm^{-1} (indicative for amorphous or highly defected crystalline MoS_2 structures) with increasing temperature (and thus increasing carbon-based content) suggests that the formation of carbon-based products hampers the self-assembly and recovery of MoS_2 layers. The recent work of Berman et al. highlights that macroscale lubricity requires the tribochemical formation of onion-like carbon structures that emerge by amorphization of nanodiamond due to the diffusion of sulfur from MoS_2 [59]. In our case, the nature of the catalytically derived carbon structures is intrinsically different to the nanodiamond used in their work [12]. Another contributing factor for the rise of COF from 0.06 to over 0.10 is the high contact pressure imparted by the Si_3N_4 ball. As thoroughly researched in our previous work [36], an increase in contact pressure resulted in a rise in friction, while for lower contact pressures, the initial low friction could be maintained or even slightly reduced. However, the intensity of the peaks characteristic for disulfides increased for higher contact pressures.

3.4. Impact of test parameters on wear

The removed wear from the Mo disk against steel balls is more pronounced when using oil with a higher S content, Fig. 4a, and at higher temperatures, Fig. 4b. The experiments at 100 °C clearly show that the oil with 1.5% EP additive allows for the same small wear volume as that without EP additive, but results in significantly lower friction coefficients, compare Fig. 1a. The oil with higher EP additive concentration leads to significantly more abrasive wear, while allowing for a similar small friction coefficient as that with 1.5% EP additive. When reducing the temperature from 100 to 40 °C (for the experiments with the 3% EP additive containing oil against steel) the wear volume massively decreases, Fig. 4b. Unfortunately, this is connected with a jump to higher coefficients of friction, compare with Fig. 2a. These results suggest that a higher rate of MoS_2 formation either supported by a higher temperature or higher additive concentration, results in a higher wear of the Mo disk. The higher wear is in part the consequence of tribochemical depletion of Mo together with a higher amount of debris that partly oxidizes to abrasive MoO_3.

When replacing the steel with a Si_3N_4 ball, the wear volume is reduced by one order of magnitude for the room temperature experiment and even two orders of magnitude for the 100 °C experiment, see Fig. 4c. The Si_3N_4 ball provides also an excellent coefficient of friction, which at room temperature is only slightly above that against steel at 100 °C, Fig. 3b. The excellent performance of the Si_3N_4 ball was also observed in our previous work, where in combination with the same EP additive lead to no wear on Mo substrates and WN coatings due to the in-situ formation of a low friction and wear protective MoS_2 or WS_2 tribofilm [36]. In the present work, another contribution could be due to the higher formation rate of C-based products when using Si_3N_4. These C-based tribofilms have been found in previous works to have low friction and also anti-wear properties [9]. In the present case, it seems that their anti-wear properties are maintained when intensively formed using Si_3N_4 at the price of hampering the low friction provided by MoS_2.

3.5. Self-assembly of MoS_2 nanoflakes in carbon tribofilms

The morphology, microstructure and chemistry of the tribofilm formed during contact between the Mo disk and the steel ball (with

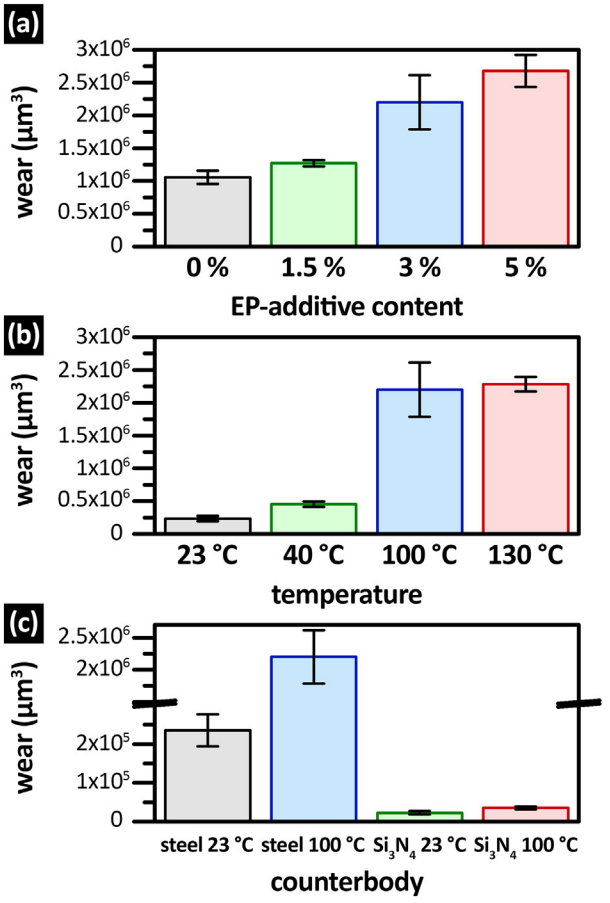

Fig. 4. Removed wear volume during lubricated reciprocating sliding of a steel ball against a mirror-polished Mo disk. Influence of (a) the EP-additive concentration in the oil during the 100 °C experiments, (b) the temperature when using a 3% EP-additive containing oil, and (c) the counterbody material for room temperature and 100 °C experiments with a 3% EP-additive containing oil.

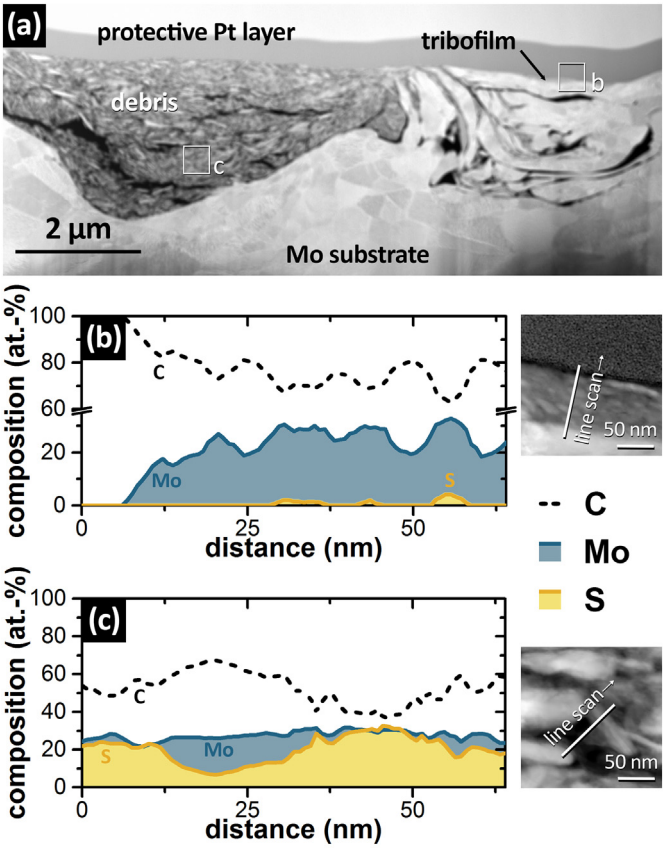

Fig. 5. Morphology and chemical composition of tribofilm and wear debris formed during contact between the mirror-polished Mo disk and a steel ball when using a 3% EP additive containing oil at 100 °C. (a) Scanning TEM overview of the FIB cross-section. (b) EELS line scan across the outermost region of the surface with a freshly formed tribofilm (as indicated in (a)). (c) EELS line scan across older buried-in wear debris particles (as indicated in (a)).

3% EP additive containing oil at 100 °C) is investigated by transmission electron microscopy of a FIB cut-out section perpendicular to the sliding direction. The scanning TEM overview image, Fig. 5a, shows the accumulated wear debris and the cross-section of the tribofilm within the groves (from the reciprocating sliding event against the steel ball) of the Mo disk. The grooved surface exhibits plastically induced grain refinement at the subsurface near regions. A significant amount of micro ploughing leads to the buildup of lamellar Mo structures (next to the grooves), which are separated by tribofilm inclusions.

An EELS line-scan across the outermost region with the tribofilm (Fig. 5b) indicates that the tribofilm basically contains carbon (derived from the oil) and Mo (from the disk), and is about 50 nm thin. While some of the Mo particles are metallic, most of them overlap with an increased sulfur signal as well, suggesting the formation of Mo–S (S from the EP additive). The EELS line scans further show that the C profile alternates with the Mo profile and the surface-near freshly formed tribofilm contains more C (Fig. 5b) than the older buried-in tribofilm particles (Fig. 5c). There, the S content even exceeds 30%, indicating a significantly higher amount of reactively formed MoS_2. This suggests that the MoS_2 formation proceeds with the number of sliding cycles.

HR TEM investigations of the buried-in wear debris region (as indicated in Fig. 5c) clearly show by selected area electron diffraction (SAED pattern given in Fig. 6a) that there are three crystalline phases: Mo debris from the sample, Fe debris from the steel ball, and MoS_2. The signals from Fe crystallites are rather weak whereas those from MoS_2 are intense. No crystalline iron sulfides could be detected, regardless of the strong affinity between Fe and S (S from the EP additive). The lack of iron sulfides in the TEM lamella is in agreement with XPS spot measurements performed on the wear track. These measurements reveal the presence of iron in metallic form and as oxide together with molybdenum in metallic and sulfide form. XPS spot analyses on the steel ball counterbody show a similar composition without the presence of iron sulfides (Table 1).

Detailed HR TEM investigations of the surface-near region with a freshly formed tribofilm (partly sandwiched between micro-ploughed lamellae), Fig. 6b, indicate small crystallites, having a lattice spacing with 2.66 Å very similar to MoS_2 (2.73 Å), see the inset in Fig. 6b. Fast Fourier Transformations of these regions also fit a MoS_2 pattern (not shown).

These investigations further proof the formation of MoS_2 during our experiments. However, also its orientation with respect to the sliding surfaces is essential, which could be identified from the wear debris area, Fig. 1c. The two facing Mo-rich surfaces are covered with layers whose lattice spacings (6.19 Å) match the (002) lattice plane distance of MoS_2 (6.15 Å). Between these surfaces, the crystalline particle with a lattice spacing of 2.67 Å again fits to MoS_2, with the (001) lattice plane distance of 2.73 Å. Corresponding MoS_2 structures were also found previously in annealed initially amorphous thin films [47]. Other regions also show 002-oriented MoS_2 layers at the Mo particle surfaces while the carbon-based regions are on top of these MoS_2 layers, Fig. 6d. This clarifies that essentially MoS_2 (and not the carbon-based regions) guarantees for easy-to-shear layers between contacting bodies. Hence, the macroscopically observed low friction merely relies on a

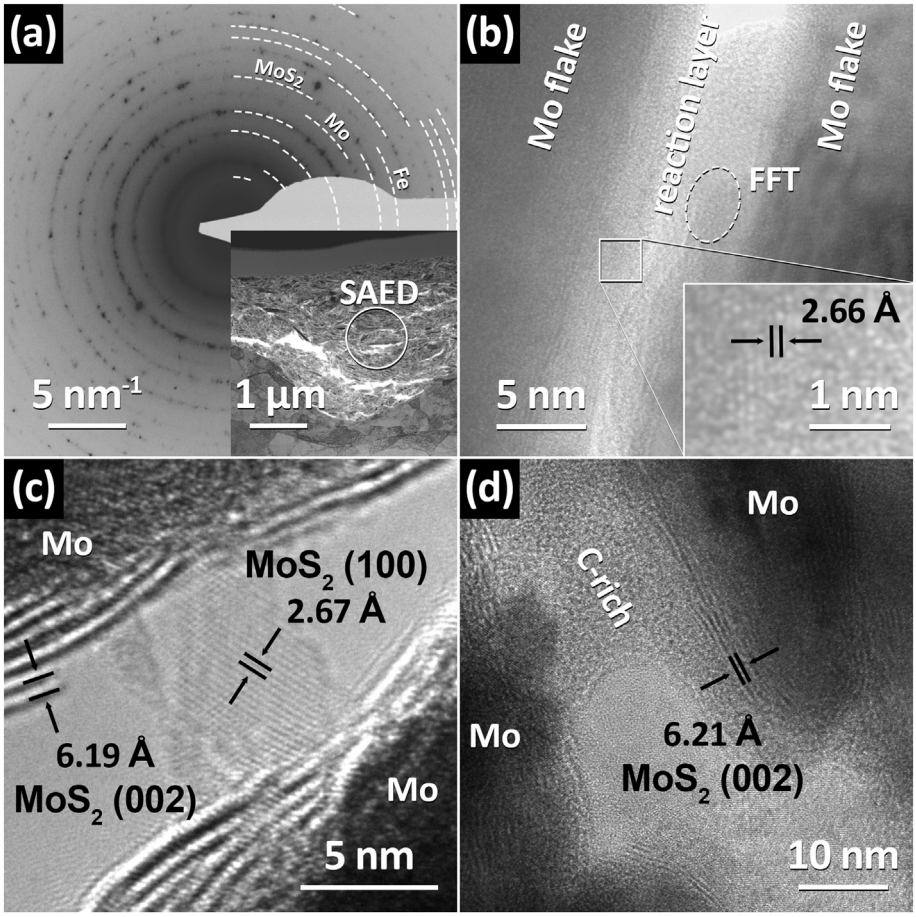

Fig. 6. HR TEM investigations of the tribofilm and wear debris formed during contact between the mirror-polished Mo disk and a steel ball when using a 3% EP additive containing oil at 100 °C. (a) SAED pattern of the debris area indicated with a dashed circle in the small inset. (b) HR TEM image of the tribofilm freshly formed at the outermost surface region indicating the area where the Fast Fourier Transformation (FFT) was performed. (c) MoS_2 layers formed on top of Mo-rich wear debris and (d) carbon-based material between MoS_2 layers covering Mo-rich particles.

few self-assembled MoS_2 monolayers formed reactively via a tribochemical reaction between Mo disk and S-containing EP additives.

4. Conclusions

Based on lubricated reciprocating sliding tests of a plain Mo disk against steel and Si_3N_4 balls we can conclude that Mo surfaces are able to catalytically decompose base oil molecules to form *sp2*-bonded carbon-based tribofilms. In the presence of S-containing EP additives (in the lubricant) the reactive in-situ formation of MoS_2 self-assembled nanoflakes is favored. We envision that the retarded breakage of hydrocarbon molecules together with a reduced catalytic activity of the Mo surface is responsible for the simultaneously observed reduced formation of oil-derived carbon products. The reason is that

Table 1
Relative surface atomic concentrations of elements found on the Mo disk and on the steel ball.

Element	State	Binding Energy (eV)	Concentration (atomic %)			
			Mo Disk (as-tested)	Mo Disk (sputtered)	Steel ball (as-tested)	Steel ball (sputtered)
S	Sulfide	161.57	7.8	12.4	17.0	20.3
	Organic	162.50	–	–	3.4	7.7
	Organic	163.34	0.8	3.8	–	2.5
	Sulfate	168.90	0.7	–	0.7	–
Mo	Metal, Carbide	227.91	2.8	16.5	1.5	9.6
	MoS_2, MoO_2	228.8	3.9	24.7	7.3	14.3
	MoO_3	232	3.4	–	–	–
C	Carbide	283.23	–	7.0	–	8.9
	C-C	284.29	42.4	6.8	46.9	4.9
	C-O	285.35	6.2	4.6	2.6	2.1
	Carbonate	288.71	2.9	–	1.8	–
O	Metallic	530.19	6.6	15.9	3.1	6.7
	Organic	531.41	17.2	5.8	11.6	5.5
Fe	Metallic	706.88	0.1	1.4	2.1	10.5
	Oxide	710.37	0.7	0.9	2.0	7.1

MoS_2 forms at the Mo surface, covering the catalytic metallic surface and also lowers the frictional energy input. While MoS_2 can already be observed in the tribofilm during the room temperature experiments, oil-derived carbon products require higher temperatures. Even though oil-derived carbon tribofilms have been reported to act as solid lubricant, in our case the only presence of C tribofilms is insufficient for decreasing friction in the absence of MoS_2. Further, in some circumstances, such as when using a Si_3N_4 counterbody, the presence of C tribofilms hampers the frictional performance of the reactively formed MoS_2 nanoflakes.

Detailed HR TEM with SAED and EELS show that the self-assembled MoS_2 layers are only a few nm thin and perfectly 002-oriented at the Mo surfaces. This guarantees for a perfect alignment of their easy-to-shear planes parallel to the sliding surfaces, enabling a low COF.

Our experiments of reciprocating sliding steel and Si_3N_4 balls against a plain Mo disk clearly show the promoted formation of MoS_2 when using steel, especially at higher temperatures and with higher EP additive containing oils. Unfortunately, this is also accompanied with a higher depletion of Mo that results in a higher wear. The harder but inert Si_3N_4 counterbodies lead to an initial COF as low as 0.06 connected with a negligible wear of the Mo disk. However, the rapidly increasing COF suggests for insufficient formation of MoS_2 or a higher removal rate. These results indicate that the removed volume is connected with the reactive in-situ formation of MoS_2. The combination of 1.5% EP additive containing oil and steel balls led to a unique performance against Mo (at 100 °C) with a COF as low as 0.08 and a hardly measurable removed wear volume.

Performing our experiments with plain Mo disks allows shedding light on the reaction kinetics and unveiling the tribochemical processes that lead to the in-situ reactive formation of MoS_2. This is essential to implement their self-assembly to other material classes like hard coatings containing Mo, as for example MoN. The results can also further used for the design of triboactive surfaces containing molybdenum or molybdenum carbides such as steels or molybdenum alloys. In all cases, the presence of Mo in the surface as carbide, nitride or in metallic form avoids the use of organometallic friction modifiers containing Mo, thus contributing towards greener lubrication.

Data availability

The raw/processed data required to reproduce these findings cannot be shared at this time as the data also forms part of an ongoing study.

Declaration of Competing Interest

The authors declare that they have no known competing financial interests or personal relationships that could have appeared to influence the work reported in this paper.

Acknowledgments

This work was funded by the Austrian COMET-Program (Project K2 InTribology, Grant No. 872176) and has been carried out within the Excellence Centre for Tribology and the TU Wien. The government of Lower Austria is gratefully acknowledged for financially supporting the endowed professorship tribology at the TU Wien (Grant no. WST3-F-5031370/001-2017) in collaboration with AC2T research GmbH. The authors acknowledge the use of facilities at the USTEM, TU Wien, Austria, and are thankful to Tomasz Wojcik for assistance with the TEM investigations.

References

[1] H. Spikes, The history and mechanisms of ZDDP, Tribol. Lett. 17 (2004) 469–489, https://doi.org/10.1023/B:TRIL.0000044495.26882.b5.
[2] N.N. Gosvami, J.A. Bares, F. Mangolini, A.R. Konicek, D.G. Yablon, R.W. Carpick, Mechanisms of antiwear tribofilm growth revealed in situ by single-asperity sliding contacts, Science 348 (2015) 102–106, https://doi.org/10.1126/science.1258788.
[3] J.M. Martin, T. Onodera, C. Minfray, F. Dassenoy, A. Miyamoto, The origin of anti-wear chemistry of ZDDP, Faraday Discuss. 156 (2012) 311–323, https://doi.org/10.1039/c2fd00126h.
[4] M.I. De Barros, J. Bouchet, I. Raoult, T. Le Mogne, J.M. Martin, M. Kasrai, et al., Friction reduction by metal sulfides in boundary lubrication studied by XPS and XANES analyses, Wear. 254 (2003) 863–870, https://doi.org/10.1016/S0043-1648(03)00237-0.
[5] A. Morina, A. Neville, M. Priest, J.H. Green, ZDDP and MoDTC interactions in boundary lubrication-the effect of temperature and ZDDP/MoDTC ratio, Tribol. Int. 39 (2006) 1545–1557, https://doi.org/10.1016/j.triboint.2006.03.001.
[6] C. Grossiord, J.M. Martin, T. Le Mogne, T. Palermo, In situ MoS2 formation and selective transfer from MoDPT films, Surf. Coat. Technol. 108–109 (1998) 352–359, https://doi.org/10.1016/S0257-8972(98)00622-7.
[7] H. Spikes, Low- and zero-sulphated ash, phosphorus and sulphur anti-wear additives for engine oils, Lubr. Sci. 20 (2008) 103–136, https://doi.org/10.1002/ls.57.
[8] M.A. Nicholls, T. Do, P.R. Norton, M. Kasrai, G.M. Bancroft, Review of the lubrication of metallic surfaces by zinc dialkyl-dithiophosphates, Tribol. Int. 38 (2005) 15–39, https://doi.org/10.1016/j.triboint.2004.05.009.
[9] A. Erdemir, G. Ramirez, O.L. Eryilmaz, B. Narayanan, Y. Liao, G. Kamath, et al., Carbon-based tribofilms from lubricating oils, Nature. 536 (2016) 67–71, https://doi.org/10.1038/nature18948.
[10] N. Argibay, T.F. Babuska, J.F. Curry, M.T. Dugger, P. Lu, D.P. Adams, et al., In situ tribochemical formation of self-lubricating diamond-like carbon films, Carbon N. Y. 138 (2018) 61–68, https://doi.org/10.1016/j.carbon.2018.06.006.
[11] B. Johnson, H. Wu, M. Desanker, D. Pickens, Y.W. Chung, Q. Jane Wang, Direct formation of lubricious and wear-protective carbon films from phosphorus- and sulfur-free oil-soluble additives, Tribol. Lett. 66 (2018) https://doi.org/10.1007/s11249-017-0945-2.
[12] H. Wu, A.M. Khan, B. Johnson, K. Sasikumar, Y.W. Chung, Q.J. Wang, Formation and nature of carbon-containing Tribofilms, ACS Appl. Mater. Interfaces 11 (2019) 16139–16146, https://doi.org/10.1021/acsami.8b22496.
[13] J.M. Martin, H. Pascal, C. Donnet, T. Le Mogne, J.L. Loubet, T. Epicier, Superlubricity of MoS2: crystal orientation mechanisms, Surf. Coat. Technol. 68–69 (1994) 427–432, https://doi.org/10.1016/0257-8972(94)90197-X.
[14] Z. Chen, X. Liu, Y. Liu, S. Gunsel, J. Luo, Ultrathin MoS2 Nanosheets with superior extreme pressure property as boundary lubricants, Sci. Rep. 5 (2015) 12869, https://doi.org/10.1038/srep12869.
[15] B.J. Irving, P. Nicolini, T. Polcar, On the lubricity of transition metal dichalcogenides: an ab initio study, Nanoscale. 9 (2017) 5597–5607, https://doi.org/10.1039/C7NR00925A.
[16] D. Berman, A. Erdemir, A.V. Sumant, Approaches for achieving Superlubricity in two-dimensional materials, ACS Nano 12 (2018) 2122–2137, https://doi.org/10.1021/acsnano.7b09046.
[17] T. Polcar, A. Cavaleiro, Review on self-lubricant transition metal dichalcogenide nanocomposite coatings alloyed with carbon, Surf. Coat. Technol. 206 (2011) 686–695, https://doi.org/10.1016/j.surfcoat.2011.03.004.
[18] T. Polcar, A. Cavaleiro, Self-adaptive low friction coatings based on transition metal dichalcogenides, Thin Solid Films 519 (2011) 4037–4044, https://doi.org/10.1016/j.tsf.2011.01.180.
[19] M. Li, Y. Zhang, P. Yu, N. Xi, Y. Wang, L. Liu, A novel and facile method for detecting the lattice orientation of MoS2 tribological surface using the SPSA process, Mater. Des. 135 (2017) 291–299, https://doi.org/10.1016/j.matdes.2017.08.067.
[20] H. Ju, R. Wang, N. Ding, L. Yu, J. Xu, F. Ahmed, et al., Improvement on the oxidation resistance and tribological properties of molybdenum disulfide film by doping nitrogen, Mater. Des. 186 (2020) 108300, https://doi.org/10.1016/j.matdes.2019.108300.
[21] M. Kalin, J. Kogovšek, M. Remškar, Mechanisms and improvements in the friction and wear behavior using MoS2 nanotubes as potential oil additives, Wear. 280–281 (2012) 36–45, https://doi.org/10.1016/j.wear.2012.01.011.
[22] J. Kogovšek, M. Kalin, Various MoS2-, WS2- and C-based micro- and nanoparticles in boundary lubrication, Tribol. Lett. 53 (2014) 585–597, https://doi.org/10.1007/s11249-014-0296-1.
[23] P. Rabaso, F. Ville, F. Dassenoy, M. Diaby, P. Afanasiev, J. Cavoret, et al., Boundary lubrication: influence of the size and structure of inorganic fullerene-like MoS2 nanoparticles on friction and wear reduction, Wear. 320 (2014) 161–178, https://doi.org/10.1016/j.wear.2014.09.001.
[24] H. Xiao, S. Liu, 2D nanomaterials as lubricant additive: a review, Mater. Des. 135 (2017) 319–332, https://doi.org/10.1016/j.matdes.2017.09.029.
[25] P. Rabaso, F. Dassenoy, F. Ville, M. Diaby, B. Vacher, T. Le Mogne, et al., An investigation on the reduced ability of IF-MoS2 nanoparticles to reduce friction and wear in the presence of dispersants, Tribol. Lett. 55 (2014) 503–516, https://doi.org/10.1007/s11249-014-0381-5.
[26] A. Tomala, M. Rodríguez Ripoll, C. Gabler, M. Remškar, M. Kalin, Interactions between MoS2 nanotubes and conventional additives in model oils, Tribol. Int. 110 (2017) 140–150, https://doi.org/10.1016/j.triboint.2017.01.036.
[27] A. Tomala, M. Rodríguez Ripoll, J. Kogovšek, M. Kalin, A. Bednarska, R. Michalczewski, et al., Synergisms and antagonisms between MoS2 nanotubes and representative oil additives under various contact conditions, Tribol. Int. 129 (2019) 137–150, https://doi.org/10.1016/j.triboint.2018.08.005.
[28] I.L. Singer, T. Le Mogne, C. Donnet, J.M. Martin, Friction behavior and wear analysis of SiC sliding against Mo in SO2 ,O2 and H2S at gas pressures between 4 and 40 Pa, Tribol. Trans. 39 (1996) 950–956, https://doi.org/10.1080/10402009608983617.
[29] B. Podgornik, S. Jacobson, S. Hogmark, Influence of EP and AW additives on the tribological behaviour of hard low friction coatings, Surf. Coat. Technol. 165 (2003) 168–175, https://doi.org/10.1016/S0257-8972(02)00766-1.

[30] V. Totolin, M. Rodríguez Ripoll, M. Jech, B. Podgornik, Enhanced tribological performance of tungsten carbide functionalized surfaces via in-situ formation of low-friction tribofilms, Tribol. Int. 94 (2016) 269–278, https://doi.org/10.1016/j.triboint.2015.08.017.
[31] I.L. Singer, T. Le Mogne, C. Donnet, J.M. Martin, In situ analysis of the tribochemical films formed by SiC sliding against Mo in partial pressures of SO2, O2 and H2S gases, J. Vac. Sci. Technol. A Vacuum Surf. Film. 14 (1996) 38–45, https://doi.org/10.1116/1.579877.
[32] W.G. Sawyer, T.A. Blanchet, Lubrication of Mo, W, and their alloys with H2S gas admixtures to room temperature air, Wear. 225–229 (1999) 581–586, https://doi.org/10.1016/S0043-1648(99)00020-4.
[33] K.K. Mistry, A. Morina, A. Erdemir, A. Neville, Tribological performance of EP lubricants with phosphorus-based additives, Tribol. Trans. 56 (2013) 645–651, https://doi.org/10.1080/10402004.2013.769288.
[34] B. Podgornik, J. Vižintin, S. Jacobson, S. Hogmark, Tribological behaviour of WC/C coatings operating under different lubrication regimes, Surf. Coat. Technol. 177–178 (2004) 558–565, https://doi.org/10.1016/S0257-8972(03)00927-7.
[35] B. Podgornik, D. Hren, J. Vižintin, Low-friction behaviour of boundary-lubricated diamond-like carbon coatings containing tungsten, Thin Solid Films 476 (2005) 92–100, https://doi.org/10.1016/j.tsf.2004.09.028.
[36] B. Kohlhauser, M. Rodríguez Ripoll, H. Riedl, C.M. Koller, N. Koutna, A. Amsüss, et al., How to get noWear? – a new take on the design of in-situ formed high performing low-friction tribofilms, Mater. Des. 190 (2020) 108519, https://doi.org/10.1016/j.matdes.2020.108519.
[37] M. Rodríguez Ripoll, V. Totolin, C. Gabler, J. Bernardi, I. Minami, Diallyl disulphide as natural organosulphur friction modifier via the in-situ tribo-chemical formation of tungsten disulphide, Appl. Surf. Sci. 428 (2018) 659–668, https://doi.org/10.1016/j.apsusc.2017.09.100.
[38] M. Rodríguez Ripoll, V. Totolin, P.O. Bedolla, I. Minami, Methionine as a friction modifier for tungsten carbide-functionalized surfaces via in situ Tribo-chemical reactions, ACS Sustain. Chem. Eng. 5 (2017) 7030–7039, https://doi.org/10.1021/acssuschemeng.7b01258.
[39] D. Wang, C. Yu, J. Ma, W. Liu, Z. Shen, Densification and crack suppression in selective laser melting of pure molybdenum, Mater. Des. 129 (2017) 44–52, https://doi.org/10.1016/j.matdes.2017.04.094.
[40] K. Leitner, P.J. Felfer, D. Holec, J. Cairney, W. Knabl, A. Lorich, et al., On grain boundary segregation in molybdenum materials, Mater. Des. 135 (2017) 204–212, https://doi.org/10.1016/j.matdes.2017.09.019.
[41] J. Cao, J. Liu, C. He, S. Li, Z. Hao, X. Xue, Enhanced ductility of W–Mo–cu alloy through the formation of nanometer-to-micrometer-thick dual-phase transition phase layer, Mater. Des. 164 (2019) 107536, https://doi.org/10.1016/j.matdes.2018.12.008.
[42] L.-L. Zhang, L. Zhang, J. Ning, Y. Sun, S. Na, On the role of pre-nitriding on improving the weldability of molybdenum alloy, Mater. Des. 198 (2021) 109377, https://doi.org/10.1016/j.matdes.2020.109377.
[43] C. Lee, H. Yan, L.E. Brus, T.F. Heinz, J. Hone, S. Ryu, Anomalous lattice vibrations of single- and few-layer MoS2, ACS Nano 4 (2010) 2695–2700, https://doi.org/10.1021/nn1003937.
[44] G.L. Frey, R. Tenne, M.J. Matthews, M.S. Dresselhaus, G. Dresselhaus, Raman and resonance Raman investigation of MoS2 nanoparticles, Phys. Rev. B - Condens. Matter Mater. Phys. 60 (1999) 2883–2892, https://doi.org/10.1103/PhysRevB.60.2883.
[45] A.P.S. Gaur, S. Sahoo, M. Ahmadi, M.J.F. Guinel, S.K. Gupta, R. Pandey, et al., Optical and vibrational studies of partially edge-terminated vertically aligned nanocrystalline MoS2 thin films, J. Phys. Chem. C 117 (2013) 26262–26268, https://doi.org/10.1021/jp407377g.
[46] H.A. MacPherson, C.R. Stoldt, Iron pyrite nanocubes: size and shape considerations for photovoltaic application, ACS Nano 6 (2012) 8940–8949, https://doi.org/10.1021/nn3029502.
[47] Z. Jin, S. Shin, D.H. Kwon, S.J. Han, Y.S. Min, Novel chemical route for atomic layer deposition of MoS2 thin film on SiO2/Si substrate, Nanoscale. 6 (2014) 14453–14458, https://doi.org/10.1039/c4nr04816d.
[48] Y.S. Min, E.J. Bae, B.S. Oh, D. Kang, W. Park, Low-temperature growth of single-walled carbon nanotubes by water plasma chemical vapor deposition, J. Am. Chem. Soc. 127 (2005) 12498–12499, https://doi.org/10.1021/ja054108w.
[49] A.C. Ferrari, J. Robertson, Interpretation of Raman spectra of disordered and amorphous carbon, Phys. Rev. B 61 (2000) 14095–14107, https://doi.org/10.1103/PhysRevB.61.14095.
[50] U.S. Schwarz, S. Komura, S.A. Safran, Deformation and tribology of multi-walled hollow nanoparticles, EPL Europhys. Lett. 50 (2000) 762, https://doi.org/10.1209/EPL/I2000-00546-1.
[51] I. Lahouij, F. Dassenoy, B. Vacher, J.M. Martin, Real time TEM imaging of compression and shear of single fullerene-like MoS2nanoparticle, Tribol. Lett. 45 (2012) 131–141, https://doi.org/10.1007/s11249-011-9873-8.
[52] J. Lara, K.K. Surerus, P.V. Kotvis, M.E. Contreras, J.L. Rico, W.T. Tysoe, The surface and tribological chemistry of carbon disulfide as an extreme-pressure additive, Wear. 239 (2000) 77–82, https://doi.org/10.1016/S0043-1648(99)00368-3.
[53] P. Nicolini, R. Capozza, P. Restuccia, T. Polcar, Structural ordering of molybdenum disulfide studied via reactive molecular dynamics simulations, ACS Appl. Mater. Interfaces 10 (2018) 8937–8946, https://doi.org/10.1021/acsami.7b17960.
[54] F. Gustavsson, S. Jacobson, Diverse mechanisms of friction induced self-organisation into a low-friction material – an overview of WS2 tribofilm formation, Tribol. Int. 101 (2016) 340–347, https://doi.org/10.1016/j.triboint.2016.04.029.
[55] P.U. Aldana, F. Dassenoy, B. Vacher, T. Le Mogne, B. Thiebaut, WS2 nanoparticles anti-wear and friction reducing properties on rough surfaces in the presence of ZDDP additive, Tribol. Int. 102 (2016) 213–221, https://doi.org/10.1016/j.triboint.2016.05.042.
[56] M. Rodríguez Ripoll, A. Tomala, C. Gabler, G. Dražić, L. Pirker, M. Remškar, In situ tribochemical sulfurization of molybdenum oxide nanotubes, Nanoscale. 10 (2018) 3281–3290, https://doi.org/10.1039/c7nr05830f.
[57] M. Rodríguez Ripoll, A.M. Tomala, L. Pirker, M. Remškar, In-situ formation of MoS2 and WS2 Tribofilms by the synergy between transition metal oxide nanoparticles and Sulphur-containing oil additives, Tribol. Lett. 68 (2020) 41, https://doi.org/10.1007/s11249-020-1286-0.
[58] L. Wang, X. Zhou, T. Ma, D. Liu, L. Gao, X. Li, et al., Superlubricity of a graphene/MoS_2 heterostructure: a combined experimental and DFT study, Nanoscale. (2017) 10846–10853, https://doi.org/10.1039/C7NR01451A.
[59] D. Berman, B. Narayanan, M.J. Cherukara, S.K.R.S. Sankaranarayanan, A. Erdemir, A. Zinovev, et al., Operando tribochemical formation of onion-like-carbon leads to macroscale superlubricity, Nat. Commun. 9 (2018) https://doi.org/10.1038/s41467-018-03549-6.